Selective Localization of a Radioiodinated Phospholipid Ether Analog in Human Tumor Xenografts

Kathleen P. Plotzke, Susan J. Fisher, Richard L. Wahl, Norman M. Olken, Scott Skinner, Milton D. Gross and Raymond E. Counsell

Departments of Pharmacology, Medicinal Chemistry, Radiology and Internal Medicine, The University of Michigan and the Division of Nuclear Medicine, VA Medical Center, Ann Arbor, Michigan

Administration of [^{125}I]-*rac*-1-O-[12-(*m*-iodophenyl)dodecyl-2-O-methylglycero-3-phosphocholine (NM-294) to athymic mice implanted with human tumors of several histologies, including adenocarcinoma of the ovary and colon, melanoma and small-cell carcinoma of the lung, resulted in excellent images of the tumors by gamma camera scintigraphy. Images of the tumor were obtained at 5 days or more postinjection, by which time nearly all background activity had cleared from the liver and gastrointestinal tract. Tumor-to-blood ratios at this time were quite high and ranged from approximately 8:1 (melanoma) to 30:1 (ovarian carcinoma), which is consistent with the scintigraphic images obtained in all human tumor models. Lipid extraction of the liver and tumor at 13 days postinjection showed that most of the radioactivity in these tissues remained associated with the parent compound, with only a small amount retained by the liver. Appropriately radioiodinated NM-294 has substantial potential as a tumor-avid radiopharmaceutical.

J Nucl Med 1993; 34:787–792

A pharmacological rationale for the design of radiopharmaceuticals involves radiolabeling pharmaceuticals that are known to act at or accumulate in specific tissues. This approach has seen extensive application in the development of tumor-avid radiopharmaceuticals (*1*). Although it is largely the radionuclide that is the diagnostic or therapeutic moiety, it is the carrier molecule which determines the distribution of the radiopharmaceutical. Studies by Snyder and co-workers demonstrated that phospholipid ethers (PLE), which are normally present in low concentrations in tissues, selectively accumulated in tumor cells as compared to surrounding normal cells (*2,3*). This metabolic difference between neoplastic and normal cells suggested a means for selectively targeting drug molecules to tumors.

In pursuit of this goal, radioiodinated analogs of these phospholipid ethers were designed and synthesized in order to evaluate their potential for use as noninvasive tumor imaging agents (*4,5*). Preliminary tissue distribution studies with [^{125}I]-*rac*-1-O-[12-(*m*-iodophenyl) dodecyl-2-O-methylglycero-3-phosphocholine (NM-294, Fig. 1) in rats bearing a Walker 256 carcinosarcoma showed the tumor to contain the highest concentration of radioactivity at 24 hr (15% of the dose) and a tumor-to-blood ratio of 13 (*6*). Scintigraphic images taken at 24 hr postinjection compared favorably with those obtained with [^{67}Ga]gallium-citrate. In contrast to the latter, however, NM-294 showed little propensity to accumulate in an inflammatory lesion in the rat. Tumor visualization was also accomplished in a rabbit bearing the Vx2 adenocarcinoma implanted intramuscularly in the thigh (*6*).

As an extension of these studies, we recently reported the synthesis and tumor-avidity of two analogs of alkylphosphocholine (APC) (*5*). These analogs (Fig. 1) were synthesized in order to evaluate the minimal structural requirements for selective tumor localization for such PLE-like compounds. Both [^{125}I]-12-[*m*-iodophenyl]-dodecyl phosphocholine (NM-324) and [^{125}I]-hexadecyl-2-(N,N-dimethyl-N-[*m*-iodobenzyl]-ammonium) ethyl phosphate (NM-326) demonstrated an ability to localize in and thereby visualize the Walker 256 tumor in rats. However, the tumor avidity of NM-324 was superior to NM-326. Moreover, preliminary studies with NM-324 showed excellent tumor localization using athymic mice bearing subcutaneous human tumors of several histologies, including ovarian adenocarcinoma, small-cell carcinoma of the lung and melanoma (*5*).

The purpose of the present study was to analyze the capacity of NM-294 to accumulate in and visualize various human tumor xenografts present in athymic nude mice.

Received Aug. 14, 1992; revision accepted Jan. 7, 1993.

For correspondence or reprints contact: Dr. Raymond E. Counsell, Department of Pharmacology, M6322 Medical Science Building I, The University of Michigan Medical School, Ann Arbor, MI 48109-0626.

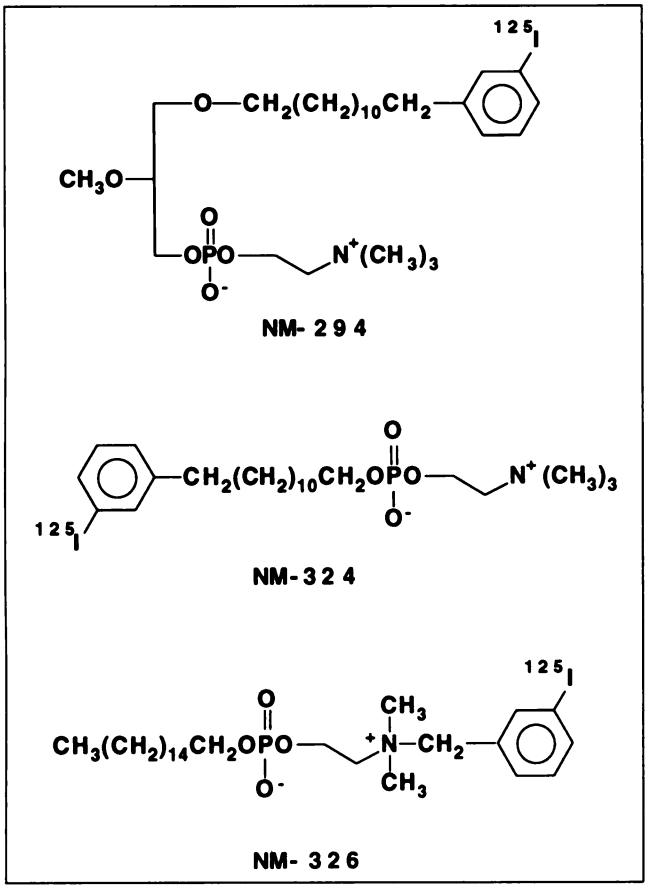

FIGURE 1. Radioiodinated phospholipid ether analogs.

MATERIALS AND METHODS

Cell Lines and Culture Conditions

NCI-H69 (human small-cell carcinoma of the lung) and HTB-77 (human ovarian adenocarcinoma) cells were purchased from ATCC (American Type Culture Collection). NCI-H69 and HTB-77 cells were maintained in RPMI 1640 medium (Sigma Chemical Co., St. Louis, MO) plus 10% fetal bovine serum (FBS) (Sigma Chemical Co., St. Louis, MO). In addition, culture medium for the human cell lines contained penicillin/streptomycin (final concentration of 50 U penicillin/ml and 50 μg streptomycin/ml) and L-glutamine, 200 m*M* (final concentration of 292 μg/ml). Cells were maintained at 37°C in a humidified atmosphere of room air supplemented with 5% CO_2.

Animal Model

Athymic nude mice (Charles River, Portage, MI), 20–25 g, were housed in specific pathogen-free rooms with free access to food and water. The mice were inoculated subcutaneously in the shoulder region with viable human carcinoma cells (1.0×10^7 cells) which were grown in tissue culture as previously described (*7,8*). These animals were used when the tumors were approximately 5 mm in diameter. The time to reach this tumor size varied with the different cell lines. For example, NCI-H69 (human small cell carcinoma of the lung) cells required 4–6 wk for tumor growth, whereas HTB-77 (human ovarian adenocarcinoma), A375 (human melanoma) and LS-180 (human colon carcinoma) took 7–14 days.

Radioiodinated Phospholipid Ether

NM-294 was synthesized as previously described (*4*). Purity and proof of structure were determined by proton nuclear magnetic resonance, infrared analysis, elemental analysis and high resolution mass spectrometry. Radioiodination with ^{125}I was accomplished by the same method as previously reported (*4*). Radiochemical purity was established by radio-thin-layer chromatography with unlabeled material serving as standard. Specific activity (S.A.) ranged from 4546 to 10,902 mCi/mmole.

Tissue Distribution Studies

NM-294 was dissolved in 95% ethanol and Tween-20 was added. The solvent was evaporated with a stream of nitrogen. Physiological saline was added in sufficient volume to give a 2% Tween saline solution. The solubilized radiolabeled compound (9.0 to 35 μCi, 0.1 ml) was administered intravenously via tail vein to tumor-bearing animals. The mice were killed at various time points by decapitation while under ether anesthesia. The blood was collected and selected tissues were removed and blotted free of excess blood. Organs were either counted whole or minced with scissors. Tissue samples were weighed in 12 × 75 mm, 5-ml plastic gamma tubes (Sarstedt, Princeton, NJ) and counted (Packard Minoxi Auto Gamma 5000). The concentration of radioactivity in each tissue was expressed as percentage of administered dose per gram of tissue.

Lipid Extraction

Samples of excised liver and tumor were homogenized in chloroform:methanol by the method of Folch et al. (*9*). Briefly, 0.1 g tissue and 0.4 ml water were homogenized in three washes of 3 ml each of chloroform:methanol (2:1 v/v) and the resulting homogenate filtered. The filter paper was air-dried and assayed for radioactivity. The filtrate was adjusted to 10 ml with chloroform:methanol (2:1 v/v) and an additional 2 ml water was added and centrifuged for 10 min at 800× g. The aqueous and organic phases were separated and the organic phase was evaporated to dryness under nitrogen. The residue was dissolved in diethyl ether and spotted on a silica thin-layer chromatography (TLC) plate with fluorescent indicator (Eastman Kodak, Rochester, NY). After allowing the plates to air-dry, they were developed in chloroform:methanol:water (65:35:6, v/v/v). The plates were removed from the developing tank, allowed to air-dry, then scanned using a System 200 Imaging Scanner (Bioscan, Inc., Washington, DC). TLC results were expressed as the percentage of the total radioactivity co-migrating with the parent compound. Additional solvent systems utilized were hexane: ethyl acetate (1:1) and chloroform:methanol:acetic acid:water (75:25:3:8, v/v/v/v). All three are well documented systems for TLC analysis of lipids (*10*).

Gamma Camera Scintigraphy

Scanning of the mice was done with a LEM Mobile Camera (Siemens Corporation, Hoffman Estates, IL) with a high-sensitivity, low-energy collimator window to detect the low-energy gamma rays of ^{125}I. Image acquisition and storage was accomplished with a Siemens MicroDELTA computer connected to a larger MicroVAX unit. Animals were sedated with 87 mg/kg ketamine and 13 mg/kg xylazine. Whole-body images (25,000 to 100,000 counts/image) were obtained at 5, 8, and 12 days following intravenous administration of 20 to 35 μCi of ^{125}I-NM-294.

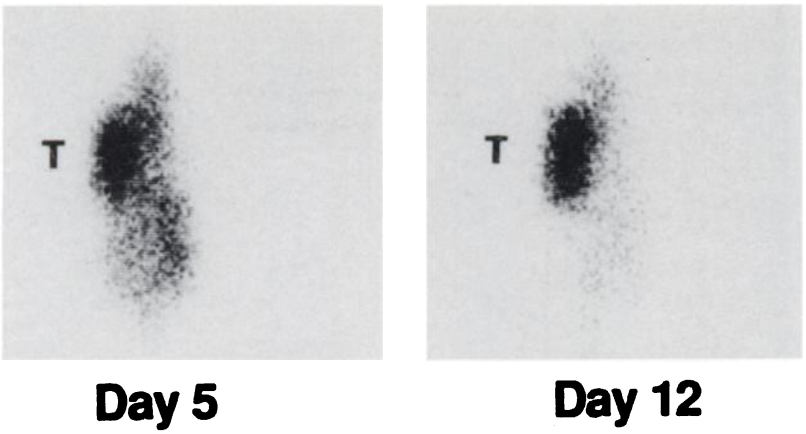

FIGURE 2. Gamma camera scintigraphy of an athymic mouse bearing a human small-cell carcinoma of the lung implanted subcutaneously in the shoulder region 5 and 12 days following intravenous administration of NM-294. The view is of the whole animal. T = tumor.

Collaborative Study

Tissue distribution studies in athymic mice with human colon carcinoma (LS-180) and melanoma (A375) were performed at NeoRx Corp., Seattle, WA. Female nude mice (bALB/c nu/nu) were purchased from Simonson Laboratories, Inc. (Gilroy, CA) and housed in microisolator caging in a controlled environment and maintained on autoclaved chow and water. The mice were implanted subcutaneously with 5×10^6 A375 (*11*) or LS-180 (*12*) tumor cells in the side midline and the tumors were allowed to grow for 1 to 2 wk to 50–200 mg. Radiolabeled NM-294 (S.A. = 417 mCi/mmole) was formulated as described above. The solubilized radiolabeled compound (2.0 μCi) was administered intravenously via tail vein to tumor-bearing animals. The mice were killed at various time points by cervical dislocation. Blood samples were collected from the retro-orbital plexus and selected tissues were isolated as whole organs, blotted, weighed and counted in a gamma scintillation well counter relative to a fractional standard of the injected dose. The concentration of radioactivity in each tissue was expressed as a percentage of the injected dose per gram (%ID/g) of tissue.

RESULTS AND DISCUSSION

To evaluate the potential of NM-294 as a tumor imaging agent in human cancer, gamma camera scintigraphic images were obtained in athymic mice bearing subcutaneous human tumors, NCI-H69 (small-cell carcinoma of the lung) and HTB-77 (ovarian adenocarcinoma). The scans obtained at 5 days postinjection in the mice bearing the small-cell carcinoma of the lung showed tumor localization of the compound, but revealed a relatively high background activity level (Fig. 2). By 12 days, the background activity had cleared from the principal nontarget tissues (liver and gastrointestinal tract) to provide excellent images of the tumors (Fig. 2). Tissue distribution data obtained on these mice following the last day of imaging was consistent with the gamma camera results which demonstrated the tumor to have the highest concentration of radioactivity, with a tumor-to-blood ratio of 25:1 (Fig. 3). A similar pattern was seen in the mice bearing ovarian carcinoma at 5 days postinjection (Fig. 4).

Lipid extraction of the liver and tumor demonstrated that most (>75%) of the radioactivity present was lipid extractable. TLC of the organic phase showed that radioactivity remaining in the tumor in each case was associated with the parent compound (Fig. 5). Additional analysis in other solvent systems (see Methods) confirmed the presence of only parent compound (data not shown).

Tissue distribution studies in nude mice with ovarian adenocarcinoma (HTB-77) correlated well with the scintigraphic studies (Table 1). At early time points (1–12 hr), most of the radioactivity was located in the liver, small intestine and kidney. For example, the liver contained 34.01 ± 4.1 %ID/g at 1 hr postinjection but decreased rapidly to 3.99 ± 0.38 %ID/g by 24 hr. In contrast, the tumor demonstrated an initial uptake of radioactivity that remained fairly constant up to 8 days postinjection. In

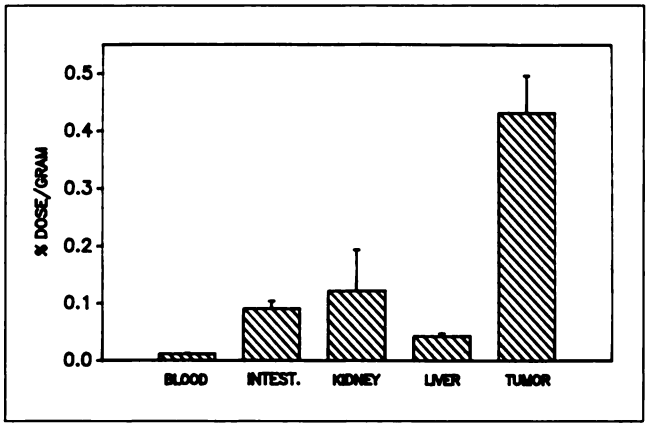

FIGURE 3. Tissue distribution of radioactivity following intravenous administration of NM-294 in athymic mice bearing small-cell carcinoma of the lung 13 days postinjection. The data are expressed as %ID/g of tissue ± s.e.m.

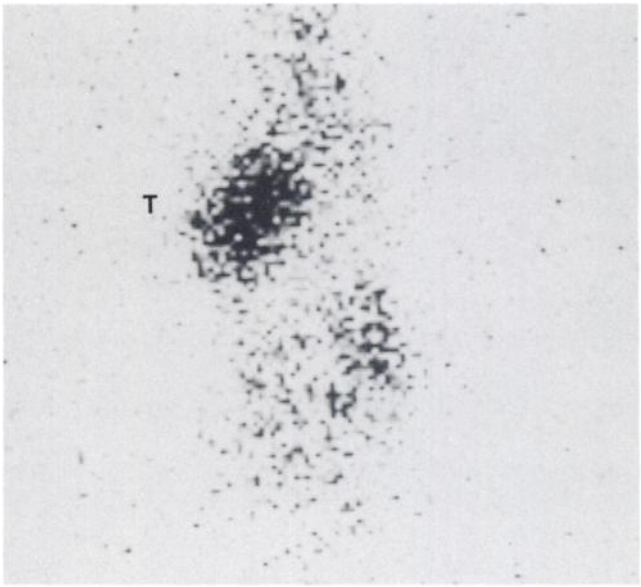

FIGURE 4. Gamma camera scintigraphy of an athymic mouse bearing a human ovarian adenocarcinoma implanted subcutaneously in the shoulder region 5 days following intravenous administration of NM-294. The view is of the whole animal. T = tumor.

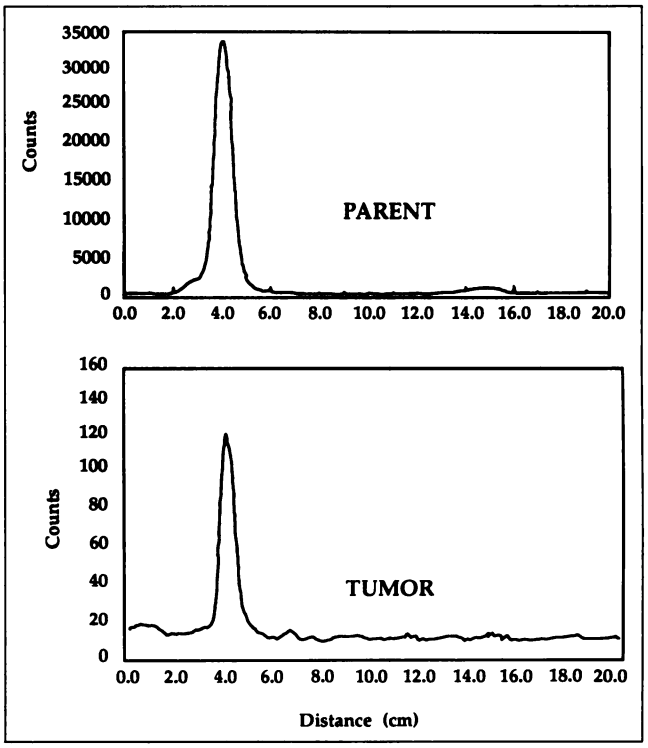

FIGURE 5. Thin-layer chromatography of lipid extracts of the dose injected (parent) and of a tumor from an athymic mouse with small-cell carcinoma 13 days postinjection. The solvent system employed was chloroform:methanol:water (65:35:6, v/v/v) and the origin and solvent front were at 2.8 and 17.0 cm, respectively.

addition, there was a high level of radioactivity in the small intestine appearing after a lag period of about 4 hr, almost certainly due to hepatobiliary clearance. This intestinal activity could account for the high abdominal background seen on the scans at the earlier time points. Calculation of tissue-to-blood ratios for liver and tumor demonstrated that over time the tissue-to-blood ratio for the tumor increased while that for the liver decreased, demonstrating the relatively slow clearance of radioactivity from the tumor (Fig. 6). No significant increase in thyroid uptake was observed over time. This indicated that little, if any, dehalogenation of the labeled molecule occurred, suggesting that clearance of radioactivity from the liver and other tissues was not due to this type of metabolism.

To evaluate the high levels of radioactivity found in the small intestine, tissue distribution studies were also performed with normal nude mice. The animals were killed at 48 hr postinjection and the small intestine was removed. Radioactivity was counted in the intact intestine with contents, intestine with contents removed and intestine that had contents removed and subsequently rinsed with saline. As seen in Figure 7, most of the radioactivity resided in the contents of the small intestine. These observations, in combination with the tissue distribution studies which showed an initial high level of radioactivity in the liver with a rapid decrease, support the view that NM-294 is cleared by the hepatobiliary system in a manner similar to natural phospholipids.

In a collaborative study with NeoRx Corp., NM-294 was evaluated in athymic mice with human colon carcinoma (LS-180) and human melanoma (A375). Tissue dis-

TABLE 1
Tissue Distribution of Radioactivity in Nude Mice Bearing Human Ovarian Carcinoma Following Intravenous Administration of NM-294 (n = 3)

	1 hr		4 hr		12 hr		24 hr		3 days		5 days		8 days	
Tissue	%ID/g	s.e.m.	%ID/g	s.e.m.	%ID/g	s.e.m.	%ID/g	s.e.m.	%ID/g	s.e.m.	%ID/g	s.e.m.	%ID/g	s.e.m.
Blood	1.07	0.13	0.91	0.04	0.99	0.22	0.48	0.06	0.26	0.06	0.07	0.01	0.06	0.00
Intestine	16.67	5.10	31.50	5.37	36.92	2.45	15.37	3.45	9.28	2.43	1.58	0.50	0.90	0.04
Kidney	10.00	1.64	8.81	0.74	11.52	2.50	4.65	0.36	1.99	0.25	0.60	0.09	0.43	0.01
Liver	34.00	4.09	21.12	0.34	8.35	1.58	3.99	0.38	1.71	0.31	0.60	0.08	0.27	0.04
Tumor	1.20	0.13	1.61	0.13	1.91	0.29	2.91	0.06	2.74	0.54	2.13	0.20	3.00	0.77

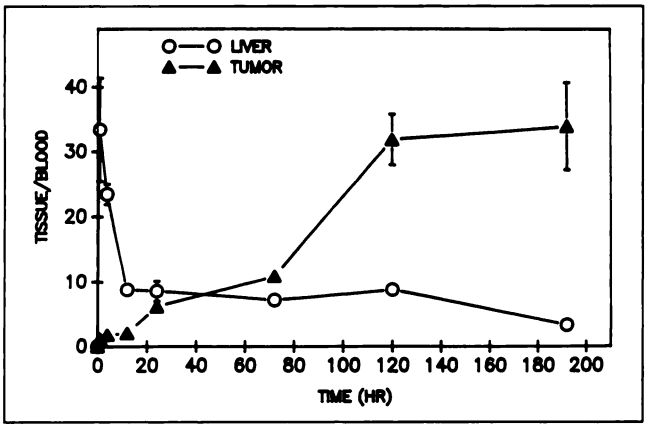

FIGURE 6. Tissue-to-blood ratios of liver and tumor from athymic mice bearing human ovarian adenocarcinoma at various times following intravenous administration of NM-294. N = three per time point.

tribution studies over a time period of 5 days in the athymic mice implanted with either colon carcinoma or melanoma showed similar results as demonstrated in our laboratory with ovarian adenocarcinoma (Table 2). At the early time points, most of the radioactivity was in the liver, but again decreased rapidly over time. By 10 hr postinjection, approximately 50% of the radioactivity present at 0.5 hr postinjection in the liver had been eliminated. Moreover, the tissue-to-blood ratios for tumor increased over time, while those for the liver diminished (Fig. 8). One methodological difference seen in this study with melanoma and colon cancer xenografts was the decrease in concentration of radioactivity in the intestinal sample. In this study, the entire intestinal tract (small and large) was removed and counted, including the contents. In contrast, in the tissue distribution studies done in our laboratory, the data represented only a portion of the small intestine. In the study with normal nude mice, the

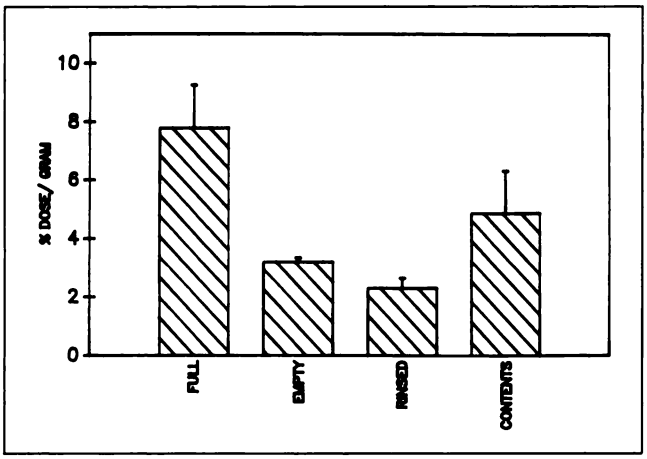

FIGURE 7. Distribution of radioactivity in the small intestines of normal athymic mice 48 hr following intravenous administration of NM-294. N = 4.

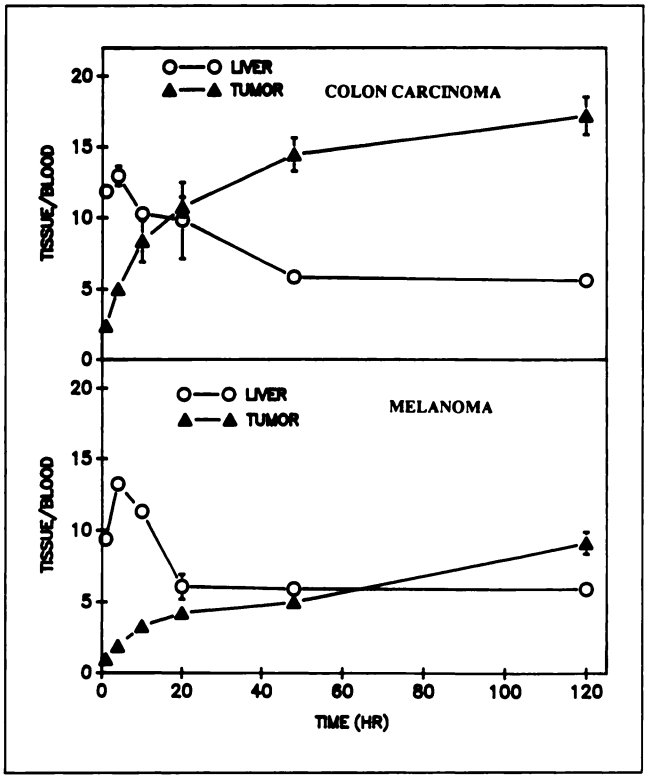

FIGURE 8. Tissue-to-blood ratios of liver and tumor from athymic mice bearing human colon carcinoma and melanoma at various times following intravenous administration of NM-294. N = four per time point.

small and large intestine (data not shown) were removed and counted. The large intestine showed significantly less radioactivity than the small intestine. A count of the entire tract therefore represents an average concentration of radioactivity found in the gastrointestinal tract and probably more accurately reflects background intestinal activity level.

When comparing the accumulation of NM-294 in the three different human tumors, there appears to be preferential tumor specificity for colon carcinoma. The %ID/g in the tumor was 5.37% (20 hr) for colon carcinoma as compared to 1.78% (20 hr) and 2.9% (24 hr) for melanoma and ovarian adenocarcinoma, respectively. In addition, the peak concentration of radioactivity in the tumor for both colon carcinoma and melanoma was achieved at 10 hr. In contrast, the peak level of radioactivity was not reached until 24 hr and remained stable up to 8 days for ovarian carcinoma. Comparison of the tumor-to-liver ratios showed that at 5 days the ratio was approximately 3:1 for both the ovarian and colon carcinomas, whereas it was only 1.5:1 for melanoma. Despite these differences in tumor uptake and clearance, there was consistency in uptake and clearance from normal tissues. For example, the %ID/g in the blood, liver and kidney for the various time points was similar for the three different human tumor models (Tables 1 and 2). These differences in the pharmacokinetics of the NM-294 in various tumor models

TABLE 2
Tissue Distribution of Radioactivity in Nude Mice Bearing Human Colon Carcinoma and Melanoma Following Intravenous Administration of NM-294 (n = 4): A Collaborative Study Performed at NeoRx Corporation

	1 hr		4 hr		10 hr		20 hr		48 hr		5 days	
Tissue	%ID/g	s.e.m.	%ID/g	s.e.m.	%ID/g	s.e.m.	%ID/g	s.e.m.	%ID/g	s.e.m.	%ID/g	s.e.m.
						Colon						
Blood	1.81	0.12	0.87	0.16	0.85	0.10	0.48	0.08	0.31	0.02	0.09	0.01
Intestine	4.60	0.33	5.70	0.89	9.96	1.09	4.79	0.12	2.24	0.21	0.53	0.07
Kidney	7.32	0.94	5.04	0.51	7.54	0.32	4.32	0.37	2.10	0.12	0.56	0.04
Liver	21.47	1.65	11.26	0.10	8.63	0.62	3.88	0.11	1.82	0.07	0.50	0.00
Tumor	4.27	0.19	4.35	0.88	6.79	1.10	5.37	1.07	4.56	0.54	1.53	0.07
						Melanoma						
Blood	2.08	0.15	1.35	0.12	0.76	0.06	0.43	0.04	0.03	0.02	0.11	0.01
Intestine	4.38	0.30	9.27	0.97	8.94	0.07	3.61	0.05	2.12	0.35	0.51	0.08
Kidney	6.89	0.60	7.68	1.06	6.34	0.05	2.39	0.04	1.77	0.14	0.67	0.02
Liver	19.40	1.40	17.83	1.54	8.51	0.05	2.68	0.06	1.69	0.10	0.60	0.01
Tumor	1.98	0.11	2.49	0.11	2.48	0.01	1.78	0.02	1.43	0.06	0.94	0.06

may be due to a number of factors that can influence uptake such as cellular growth rate, vascularity and/or blood supply of the tumor. Furthermore, differences in tumor-to-blood and tumor-to-liver ratios suggested that metabolism and clearance of this compound may also play a significant role in the degree of selective localization among the various human tumors.

CONCLUSION

Biodistribution of NM-294 in athymic mice with human tumors showed rapid elimination from the blood into the liver and then apparent redistribution into the kidney and intestine. In addition, NM-294 was accumulated and retained within various human tumors. Tumor-to-blood ratios increased at later time points, which indicate a more rapid clearance from nontarget tissue as compared to tumor. Indeed, the selective retention of radioactivity in the tumor versus nontarget tissues was sufficiently high to provide excellent gamma images of the tumor xenografts. Such results warrant further studies with NM-294 for eventual clinical evaluation.

ACKNOWLEDGMENTS

Support for this research was provided by National Institute of Health grants CA-08349 and P01-CA42768-04. The authors thank Louis Stancato, Mohamed Ruyan and Mark Rampy for technical assistance; Anaira Clavo and Gayle Jackson for assistance with cell propagation and animal inoculation; and the NeoRx Corporation, particularly Dr. Alan Fritzberg and Mr. Paul Beaumier for their assistance in the analysis of the NM-294 compound.

REFERENCES

1. Counsell RE, Korn N. Biochemical and pharmacological rationales in radiotracer design. In: Colombetti, L, ed. *Principles of radiopharmacology, volume 1*. Boca Raton, FL: CRC Press; 1979;189–250.
2. Snyder F, Wood R. The occurrence and metabolism of alkyl and alk-1-enyl ethers of glycerol in transplantable rat and mouse tumors. *Cancer Res* 1968;28:972–978.
3. Snyder F, Wood R. Alkyl and alk-1-enyl ethers of glycerol in lipids from normal and neoplastic human tissue. *Cancer Res* 1969;29:252–267.
4. Meyer KL, Schwendner SW, Counsell RE. Potential tumor or organ-imaging agents. 30. Radioiodinated phospholipid ethers. *J Med Chem* 1989;32:2142–2147.
5. Plotzke KP, Haradahira T, Stancato L, et al. Selective localization of radioiodinated alkylphosphocholine derivatives in tumors. *Nucl Med Biol* 1992;19:775–782.
6. Counsell RE, Schwendner SW, Meyer KL, Haradahira T, Gross MD. Tumor visualization with a radioiodinated phospholipid ether. *J Nucl Med* 1990;31:332–336.
7. Stya M, Wahl RL, Natale RB, Beierwaltes WH. Radioimmunoimaging of human small cell lung carcinoma xenografts in nude mice receiving several monoclonal antibodies. *NCI Monogr* 1987;3:19–23.
8. Wahl RL, Barrett J, Gealti O, et al. The intraperitoneal delivery of radiolabeled monoclonal antibodies: studies on the regional delivery advantage. *Cancer Immunoconj Immunother* 1988;26:187–201.
9. Folch J, Lees M, Sloane Stanley GH. A simple method for the isolation of total lipides from animal tissues. *J Biol Chem* 1957;226:497–509.
10. Stein J, Smith G. Phospholipids. *Techniques in Lipid and Membrane Biochemistry* 1982;B403:1–15.
11. Beaumier PL, Morgan AC. Melanoma: the development of immunoconjugates from a preclinical viewpoint. In: Herberman RB, Mercer DW, eds. *Immunodiagnosis of cancer*. New York: Marcel Dekker, Inc.; 1990: 297–316.
12. Tom BH, Rutzky LP, Ouasu R, Tomita JT, Goldenberg DM, Kahan BD. Human colon adenocarcinoma cells. II. Tumorigenic and organoid expression in vivo and in vitro. *J Natl Cancer Inst* 1977;58:1507–1512.